Published in final edited form as:
Retina. 2013 February ; 33(2): . doi:10.1097/IAE.0b013e31827e25e0.

Subretinal Drusenoid Deposits In Non-Neovascular Age-Related Macular Degeneration: Morphology, Prevalence, Topography, And Biogenesis Model

Christine A. Curcio, PhD[1], **Jeffrey D. Messinger, DC**[1], **Kenneth R. Sloan, PhD**[2], **Gerald McGwin, PhD, MS**[3], **Nancy E. Medeiros, MD**[4], and **Richard F. Spaide, MD**[5]

[1]Department of Ophthalmology, University of Alabama at Birmingham, Birmingham AL

[2]Department of Computer and Information Science, University of Alabama at Birmingham, Birmingham AL

[3]Department of Epidemiology, University of Alabama at Birmingham, Birmingham AL

[4]Retina Specialists of North Alabama, Huntsville AL

[5]Vitreous Retina Macula Consultants of New York, New York NY

Abstract

Purpose—To characterize the morphology, prevalence, and topography of subretinal drusenoid deposits (SDD), a candidate histological correlate of reticular pseudodrusen, with reference to basal linear deposit (BlinD), a specific lesion of age-related macular degeneration (AMD); to propose a biogenesis model for both lesions.

Methods—Donor eyes with median death-to-preservation of 2:40 hr were post-fixed in osmium tannic acid paraphenylenediamine and prepared for macula-wide high-resolution digital sections. Annotated thicknesses of 21 chorioretinal layers were determined at standard locations in sections through the fovea and the superior perifovea.

Results—In 22 eyes of 20 Caucasian donors (83.1 ± 7.7 years), SDD appeared as isolated or confluent drusenoid dollops punctuated by tufts of RPE apical processes and associated with photoreceptor perturbation. SDD and BlinD were detected in 85.0% and 90.0% of non-neovascular AMD donors, respectively. SDD was thick (median, 9.4 μm) and more abundant in perifovea than fovea ($p<0.0001$). BlinD was thin (median, 2.1 μm) and more abundant in fovea than perifovea ($p<0.0001$).

Conclusion—SDD and BlinD prevalence in AMD eyes are both high. SDD's organized morphology, topography, and impact on surrounding photoreceptors imply specific processes of biogenesis. Contrasting topographies of SDD and BlinD suggest relationships with differentiable aspects of rod and cone physiology, respectively. A 2-lesion, 2-compartment biogenesis model incorporating outer retinal lipid homeostasis is presented.

Corresponding Address: Christine A. Curcio, PhD, Department of Ophthalmology, EyeSight Foundation of Alabama Vision Research Laboratories, 1670 University Boulevard Room 360, University of Alabama School of Medicine, Birmingham AL 35294-0099, Ph 205.996.8682; F 205.934.3425, curcio@uab.edu.

Keywords

age-related macular degeneration; basal linear deposit; cholesterol; fovea; histopathology; lipoproteins; macula; photoreceptors; reticular drusen; subretinal drusenoid deposit

Introduction

A lesion recently recognized in eyes with age-related macular degeneration (AMD) is subretinal drusenoid deposit (SDD) [1]. Clinicopathologic studies by the Sarks showed that membranous debris, the principal component of soft drusen and basal linear deposit (BlinD), is also found in vacuoles within the retinal pigment epithelium (RPE), basal mounds within basal laminar deposit (BlamD), and within the subretinal space [2, 3]. The subretinal material was named SDD by one of us (CAC). SDD shares with soft drusen superficial ultrastructural and compositional similarities, including membrane-bounded particles with neutral lipid interiors, unesterified cholesterol (UC), apolipoprotein E (apoE), complement factor H, and vitronectin [2-6]. Conversely, SDD lacks immunoreactivity for photoreceptor, Müller cell, and RPE marker proteins. SDD of lateral length 12-190 μm was present in 9% and 22% of two small series of non-neovascular AMD eyes, respectively [4, 7]. Because eyes in these histological studies were non-exhaustively sectioned, SDD width and prevalence may have been underestimated.

SDD has been linked to the phenotype reticular pseudodrusen, a lesion variably named and described, depending on the imaging modality, patient population, and investigators. First shown in blue reflectance photography [8], pseudodrusen visible in the blue channel of color fundus photographs and in near-infrared reflectance images were attributed to SDD in our previous studies, which revealed discrete collections of hyper-reflective material in the subretinal space by spectral domain optical coherence tomography (SD-OCT) [1, 9]. In an early direct clinicopathologic correlation, the Sarks attributed reticular pseudodrusen seen in red-free photography or infrared reflectance to choroidal fibrosis in an AMD specimen lacking neurosensory retina [10]. They later changed this attribution to SDD after reviewing another specimen with an attached retina [11].

More information about the histopathology of SDD would facilitate understanding of its role in AMD pathophysiology, including its relationship with AMD's signature sub-RPE lesions. Here we report SDD morphology, prevalence, and topography in donor eyes meeting histopathologic criteria for non-neovascular AMD. To provide insight into SDD pathogenesis, we compared it to BlinD, a specific accumulation of material under the RPE in AMD that also forms mounds seen clinically as soft drusen. [2, 12] We analyzed lesion morphology in systematically sampled high-resolution histological cross-sections of whole macula [13]. We find that SDD is robust and as prevalent as BlinD, and located preferentially in the perifovea, in contrast to BlinD's predilection for the fovea. These distinct lesion topographies plausibly reflect differential aspects of rod and cone photoreceptor physiology.

Methods

This study used donor eyes accessioned for research from the Alabama Eye Bank (1995-2008). Median death-to-preservation time was 2:40 hr. Eyes were preserved by immersion in 1% paraformaldehyde and 2.5% glutaraldehyde in 0.1M phosphate buffer following anterior segment removal. Donor eyes with gross macular appearance consistent with early AMD and unremarkable maculas from age-matched donors were sectioned and evaluated (n=64 total). Maculas with retina in place and vitreous removed were subjected to *ex vivo* color photography with a dissection scope [14]. Tissue was post-fixed by osmium

tannic acid paraphenylenediamine for neutral lipids in extracellular AMD-associated lesions [1516]. Macula-wide, high-resolution sections were collected starting at the superior edge of an 8 mm diameter full-thickness punch [13, 17] and stained with toluidine blue (Figure 1). Study sections were 2 mm superior the foveal center, i.e., within superior perifovea, where reticular pseudodrusen are abundant clinically, and in the foveola.

Clinical records were available for some donors, but not all. AMD case ascertainment used histopathologic criteria [1418]. Criteria for non-neovascular AMD were a foveolar section lacking evidence of choroidal neovascularization or a fibrovascular scar AND either a druse >125 μm OR severe RPE change (hyperplasia, multiple layers, anterior migration) AND either drusen OR continuous basal laminar deposit (BlamD) [143, 19].

The use of digital sections scaled to tissue units (μm), a fovea-centered coordinate system, and systematic sampling enabled comparisons of morphological data across eyes and inference about the extent of macula affected by lesions. Sections were scanned with a 40× numerical aperture 0.95 objective, a robotic microscope stage, and image-stitching software (CellSens, Olympus). Digital sections (~500 MB) were used for recording annotated thicknesses of chorioretinal layers [13]. Using custom plug-ins written for ImageJ (http://rsbweb.nih.gov/ij/), a single experienced observer (CAC) sampled maculas at 25 locations from 3 mm nasal to 3 mm temporal. Thirteen locations were ≤1 mm of the foveal center where neurosensory retina cell density gradients change rapidly [20, 21]. At each location, layer thicknesses were measured using the Segmented Lengths tool, and layer-appropriate annotations chosen from a menu. RPE morphology and pigmentation was graded on an 8-point scale adapted from [22, 23].. Glass slides were viewed with a 60× oil-immersion objective (numerical aperture = 1.4) in parallel with digital sections to inform judgments about small structures. Thicknesses and annotations were extracted by custom ImageJ plug-ins for analysis with spreadsheets (Microsoft; Excel 2008) and statistical software (SAS, Cary NC; StatPlus for Mac). Thicknesses accumulated relative to the RPE basal lamina were displayed as layer plots (Figure 2).

Thicknesses are reported for the subretinal space, RPE, BlamD, sub-RPE space, and choriocapillaris. In this post-mortem material, neurosensory retina was detached at 72.7% of SDD-containing locations. Detachment may be accompanied by compaction of RPE apical processes into a layer of relatively uniform thickness. Alternatively, RPE apical processes may be upright and individually resolvable where pulled by detaching retina [22, 24]. Even in attached specimens, outer segments were frequently compacted. Although these factors can compromise SDD morphology and impair its recognition, histological sections were interpretable. Only a solid flocculent material that also appeared in attached specimens was called SDD. Other materials in the subretinal compartment, including isolated cells, oil droplets, pigment granules, and a fine proteinaceous substance, were distinguishable from SDD. Scattered or loosely packed SDD-like components, or empty spaces between fascicles of RPE microvilli were not called SDD. Because it is possible that other SDD forms did not survive processing, our estimates of SDD thickness, coverage, and prevalence should be considered lower bounds. Accordingly, we did not adapt a SD-OCT grading scale for SDD and SDD-associated outer retinal hyper-reflective band deflections [1] to histological sections.

Within the sub-RPE compartment, a grayish-pink layer of non-uniform thickness was called BlinD (Figure 3B,C arrowheads) and distinguished from a grayish-pink layer of uniform thickness (Figure 3C, arrows) thought to represent stacked lipoprotein particles on the inner surface of Bruch's membrane of many older eyes [15, 25, 26]. Other sub-RPE components included drusen, presumed Müller cells extending externally from the Henle fiber layer in neurosensory retina [27], pigment-containing cells, and fluid.

Lesion prevalence was determined from thicknesses measured at sampling locations. Sampling locations were classified as SDD Only, BlinD Only, both SDD+BlinD, or Neither Lesion, and associations of these lesions with RPE status and BlamD thickness at the same eccentricity was computed. In the analysis of macular subregions, locations ≤0.6 mm from the foveal center on the section through the foveola were called Fovea. Those on either side were Nasal or Temporal perifovea. In sections through Superior perifovea, the percentage of RPE-BrM length covered by SDD (coverage) was computed.

Morphometric characteristics were compared between lesion groups using mixed statistical models and generalized estimating equations for continuous (e.g., BlamD thickness) and categorical (e.g., RPE pathology grade) variables, respectively, to account for data clustering (i.e., multiple sections from individual eyes and the fellow eyes). Calculation of lesion prevalence on a per donor basis included only one eye per donor.

Results

Study eyes

Results are presented from 22 eyes of 20 Caucasian donors (14 female, 6 male, mean age 83.1 ± 7.7 yr) at early (n=17) and advanced (n=5) stages of non-neovascular AMD. Five of 9 donors with clinical histories were diagnosed with non-neovascular AMD 2.1 to 41.2 mo prior to death. Others had clinically unremarkable maculas.

SDD morphology

SDD was found as either isolated or confluent drusenoid mounds or dollops[9]. Figure 4A shows isolated SDD, which dominate in the valleys between conventional drusen. The middle formation in Figure 4A has an apical cap of medium staining and irregular oval inclusions ∼1 μm in diameter, superficially resembling a condensate of outer segment-like material [28] but lacking internal structure resembling disks. Other nearby formations lacking this cap have internal septa. In this specimen with an attached retina, photoreceptor morphology is disturbed over all SDD formations, manifest as outer segment (OS) shortening (Figure 4A, **#1 and 3**) and OS loss with inner segment deflection and absence (Figure 4A, **#2**). The largest SDD encroached on photoreceptors, apparent even in detached retinas, in which the border formed by OS tips was scalloped rather than straight (not shown), and the lesion itself was decapitate. Figure 4B shows the best-preserved example of perifoveal SDD in an eye where the retina is not only attached but the photoreceptors are upright and closely apposed to the SDD internal surface. Here, confluent SDD have septae of fasciculated apical processes (arrows).

Further details of sheet-like SDD morphology are shown in Figure 5. A formation in superior macula resembling reticular pseudodrusen (“ill-defined networks of broad interlacing ribbons” [29]) was apparent in *ex vivo* color photographs of one eye (Figure 5A) but not its fellow (Figure 5B) or others, presumably due to post-mortem opacification of neurosensory retina. Apical processes in SDD-bearing eyes form regularly spaced bundles resembling uplifted arms along a scalloped RPE surface (Figure 5C,D). Photoreceptor OS, mostly rods, appear associated with microvilli bundles, wrapping around SDD mounds to reach the RPE, as described [7] Shortened photoreceptors abut SDD's inner surface, between bundles (Figure 5G). The narrowest SDD material visible by light microscopy in specimens with attached retinas or in sites where SDD was clearly delimited by microvilli bundles and associated OS tips is 8-17 μm, similar to the width of 1-2 RPE cells (Figure 5F). Whether this implies that some RPE do not touch photoreceptors is not certain, as SDD may contain tufts of apical processes visible in other sections. Perifoveal SDD were seen to be quite extensive. Median coverage of RPE by SDD in Superior perifovea of 20 eyes was 20.3%

(section length 6.70 ± 0.70 mm). Five eyes had SDD coverage of ≥62.4%. In Figure 6, SDD overlies numerous partially intact soft drusen containing neutral lipid pools and additionally lies within inter-druse valleys.

SDD fine structure is similar but not identical to the contents of soft drusen, BlinD, and basal mounds, the classically described sites of membranous debris [2] (also called lipoprotein-derived debris [30]). In Figure 5C, SDD is packed with membranous profiles. In Figure 5D, SDD comprise a dispersed phase of deeply stained particulate material within a flocculent continuous phase. In these eyes different compositional textures appear to vary on an eye-by-eye basis, i.e., SDD with particulate interiors are found throughout that section. These findings may be due to between-eye differences in preservation quality or more intriguingly, to a distinct taxonomy of SDD morphological phenotypes, like that described for conventional drusen.

Lesion prevalence, topography, relationship to other AMD pathology

Median SDD thickness was 9.4 μm (range, 3.4-51.1 μm; Q1=6.2 μm; Q3=13.6). Median BlinD thickness was 1.8 μm (range, 0.5-34.4 μm; Q1=1.1 μm; Q3=4.6). SDD was significantly thicker than BlinD (t-test for unequal variances, $p<0.0001$).

Annotated layer thicknesses obtained through systematic sampling of retinal regions were used to quantify SDD and BlinD prevalences, topography, and lesion associations with other aspects of AMD pathology. Of 20 non-neovascular AMD donors covered by 1,000 sampling locations, 17 (85.0%) had SDD, and 18 (90%) had BlinD, at any location. Under a stricter criterion of at least 3 affected locations per eye, SDD was present in 14/20 (70.0%), and BlinD, 13/20 (65.0%) of AMD donors. Individuals varied considerably in lesion extent, from 1-25 affected locations per eye for SDD (mean, 9) and 1-22 for BlinD (mean, 7). Variability in SDD and BlinD extent was not correlated ($p=0.23$).

A striking observation was the abundance of BlinD and paucity of SDD in the fovea, and the abundance of SDD in the Superior perifovea (Table 1). Of sampling locations with SDD only, 9.9% were in the Fovea, and 90.1% were in the perifovea, in the order Superior (62.0%) ≫ Nasal (17.5%) > Temporal (10.5%) ($p<0.0001$ for difference among regions; inferior retina was not sectioned). Of sampling locations with BlinD only, 57.1% were in the fovea and 42.9% in the perifovea with similar proportions (12.0-15.8%) in Nasal, Superior, and Temporal subregions. Topographies were also assessed by calculating the percentage of sampling locations in each macular subregion, i.e., normalizing with respect to region rather than by lesion group (Figure 7). This analysis shows that 34.5% of foveal locations had BlinD, compared to only 4.0-15.0% of perifoveal locations. Conversely, 12.9-21.4% of perifoveal locations had SDD, compared to only 7.7% of foveal locations. Pooling locations with drusen with those containing only BlinD did not change this conclusion (data not shown). A second striking observation is that any one location tended to have either SDD (17.1% of total locations) or BlinD (13.3%), but not both (only 2.3%). Thus, even in regions of topographic overlap, SDD and BlinD tend not to appear on opposite aspects of the same RPE cells, as previously noted [11]. Finally, both pairs of fellow eyes had highly concordant findings of abundant SDD and minimal BlinD.

We examined other aspects of AMD pathology at sampling locations with SDD, BlinD, or neither lesion. RPE morphology ranged from unaffected to atrophic (absence of a pigmented layer, with or without BlamD, Table 1) in these non-neovascular AMD eyes. RPE morphology was worse in locations with either SDD or BlinD compared to locations with neither lesion ($p<0.0001$). More locations with BlinD only were associated with atrophic RPE (14.0%) than with SDD only (0.6%; $p=0.0036$). BlamD, considered a marker of AMD progression [3], was present at 76.8% of locations with SDD only and 81.5% of locations with

BlinD only. BlamD was thicker (6.2 μm) at locations associated with BlinD than at locations associated with SDD only (4.2 μm) ($p<0.03$). Finally, we checked for vascular changes associated with SDD and BlinD. Choriocapillary ghosts are recognized readily by the absence of endothelial cells in an arch-like space delimited by intercapillary pillars [31, 32]. Ghosts were present in similar proportions at locations with SDD+BlinD and with neither lesion (7.7 and 8.7%, respectively, Table 1). They were higher in areas with either lesion, especially sites with BlinD only (17.3%). We also examined the choroid external to these lesions for signs of vascular sclerosis [10] or other abnormalities, and primarily noted overall choroidal thinning, loss of large vessels, and hyalinization of stroma throughout the macula.

Discussion

This is the largest series of eyes devoted to histological characterization of SDD and the first study to compare thicknesses and topographies of AMD-specific lesions. We solidify previous observations from smaller series of AMD and non-AMD eyes [2, 4, 6, 7, 11, 28] that SDD is an organized and stereotypical lesion that is readily distinguishable from other subretinal components and from extracellular lesions in other compartments. Its association in attached retinas with deflected and shortened photoreceptors supports the idea that the lesions are in place during life and are not relocated by processing artifact [28, 33]. Our principal new finding is SDD preferentially localizes to the perifovea, a location where there is a high density of rods whereas BlinD is thickest in the fovea, where there is a high density of cones [21] (Figure 8). Results suggest that SDD and BlinD reflect differential aspects of rod and cone physiology, linking macular photoreceptor topography and AMD pathology.

SDD and BlinD are both common in non-neovascular AMD, yet SDD has come to the fore only recently. SDD's first two histological descriptions were separated by 15 years and pertained to two different diseases [2, 28]. The first two descriptions in AMD eyes were separated by 17 years [2, 4]. SDD was not reported in histological surveys of AMD eyes using paraffin [19, 34, 35] or cryo-sections [36-38], likely because its optimal visualization requires osmium post-fixation, semi- or ultra-thin sections, and samples that include non-foveal macula. Ultrastructural studies, including our own, tended to concentrate on fovea [2, 3, 5, 12, 39, 40] or did not specify sample location [41]. Finding SDD requires looking for it, and seeing it in enough attached specimens to enable informed interpretation of detached specimens, which, in turn, implies tissues obtained quickly after donor death. In this study we used high-resolution sections of short post-mortem (<3 hr) tissues post-fixed to preserve neutral lipids in AMD's characteristic lesions. Finally, SDD's significance became apparent only when new clinical imaging technologies such as spectral domain optical coherence tomography enabled visualization of a widely distributed lesion with a distinctive morphology, topography, and independent risk levels for progression [1, 42, 43].

A major question is whether SDD accounts for the clinical appearance of pseudodrusen described by different investigators using various high-resolution instruments. Several salient features of reticular pseudodrusen can be related to our current or past [7] histological data: **1)** Descriptions of interlacing yellow material or networks [2944]. **2)** High prevalence in AMD eyes, especially geographic atrophy [45], with prevalence estimates varying widely with detection method [45] and patient population (Table 2). **3)** Bilateral symmetry [42, 46]. **4)** Abundance in superior and superior temporal macula, with more outside the macula superiorly [1, 10, 29, 47-49] and little [10, 47] in central macula. **6)** Dynamism over time, with expansion into superior retina [1011] and continuous focal enlargement and anterior migration into the retina [50]. It would be remarkable with this level of correspondence if SDD were not the histological correlate of reticular pseudodrusen, as it would imply that another feature of this magnitude in the same region remains to be detected clinically. Further, the varying clinical appearances, ranging from dots to ribbons, raise the possibility of multiple SDD

subtypes or stages of progression or both, with distinctive ultrastructural correlates and compositions. The name reticular pseudodrusen appears inappropriate for this lesion, which is neither universally reticular (network), pseudo (false), nor drusen (sub-RPE).

A comprehensive theory of AMD extracellular lesion formation would ideally account for both SDD and sub-RPE drusen/ BlinD. An existing model for BlinD involving its largest component, cholesterol-rich lipoproteins containing apolipoproteins B and E [30, 51] is summarized as **steps 1-4** in Figure 9. We hypothesize that the RPE is a polarized and bidirectional secretor of lipoproteins which serve photoreceptor and RPE physiology driven by OS membrane lipid composition, and that these lipoproteins participate in lesion formation in two compartments, as follows.

Strong circumstantial evidence suggests that one or more HDL (high-density lipoprotein) classes subserve intra-retinal lipid transport, including a rapid distribution of lipoprotein-delivered UC from the choroid into neurosensory retina [52]. HDL are multifunctional, multimolecular assemblies consisting of an esterified cholesterol (EC)-rich core solubilized by surface components of apolipoproteins and phospholipids. Plasma HDL, 7-11 nm in diameter, is notable for multiple classes defined by different isolation techniques and by extensive extracellular remodeling via enzymes and transfer proteins. These include lecithin acyl cholesterol transferase (LCAT), cholesterol ester transfer protein (CETP), phospholipid transfer protein (PLTP), hepatic lipase (LIPC) [53, 54]. In reverse cholesterol transport, plasma HDL receives UC from cellular membranes throughout the body via ATP binding cassette A-I (ABCA-1) for transport to liver, where scavenger receptors (SRB-I, II) mediate selective EC uptake. HDL carries >100 proteins, including complement factors and coagulation factors. Fewer than half subserve lipid metabolism [55]. Brain cerebrospinal fluid, embryologically equivalent to the subretinal space, also harbors HDL-like lipoproteins containing apoE. These serve the rich lipid traffic between astrocytes and neurons, subject to remodeling via intracerebrally expressed LCAT, CETP, and PLTP [56-58]. Of relevance to SDD, variants in CETP and LIPC genes modify AMD risk independent of plasma HDL levels [59-61]. ApoE, CETP, LIPC, LCAT, and SRB-II immunoreactivity, along with PLTP activity, localize to interphotoreceptor matrix [52, 62]. ApoE is secreted by RPE and Müller cells, appearing in aspirates from rhegmatogenous retinal detachments [63-67]. SDD contains complement cascade components and regulators [7, 68]. Thus numerous molecules with well-known HDL associations are present in the subretinal space.

Rod OS disks pinch off from the plasma membrane near the inner segment. They become internal membranes, which unlike plasma membranes, are low in UC content (10% vs 30-35%) [6970]. In transit from OS base to tip, [71] disks reduce UC and increase the fatty acid docosahexaenoate (DHA) within phospholipids (**step 5,** Figure 10). These changes enable the conformational flexibility of rhodopsin required by single-photon sensitivity. OS-derived DHA stored in RPE after disk shedding and phagocytosis are recycled back to inner segments [72, 73] by an as-yet unspecified mechanism. HDL particles cycling between RPE and photoreceptors, proposed for intra-retinal lipid transfer to inner segments [52], could move both UC from, and DHA to, OS disks progressing toward the RPE. In contrast (**step 6,** Figure 10), cone OS disks are comb-like projections of plasma membrane and are believed to maintain high UC content along their length (unpublished observations; personal communication, R. Mullins, 5/9/12) [71]. Cone OS UC enters RPE via disk shedding and lysosomal uptake. This UC is released for intracellular transfer, esterification, and assembly into basolaterally-secreted apoB,E-containing lipoproteins, especially under cone-dominant fovea, where they form the basis of BlinD (**Step 3, 4,** Figure 10). Using perturbation of cholesterol homeostasis and lipid transfer as unifying mechanisms, it may be possible to explain the formation of SDD in areas enriched with rods and BlinD under the cone-

dominant fovea, with downstream negative consequences such as inflammation, in both compartments.

Strengths of this work include short post-mortem donor eyes, time-of-study histopathologic AMD ascertainment as opposed to clinical histories obtained at variable pre-mortem intervals, a tissue preparation technique designed to improve neutral lipid preservation, a quantized RPE grading scale, and a retina-centered coordinate system and systematic sampling that together facilitated statistical analysis across eyes. Limitations include post-mortem retinal detachment, absence of extensive serial section reconstruction, limited clinical histories that did not include imaging or genotype, and the subjective nature of histological judgments.

Reflecting remarkable compartmentalization of photoreceptor, RPE, and Bruch's membrane functions, AMD's lesions reflect different biological pathways deployed with micrometer precision in the vertical axis. BlinD and soft drusen are external to RPE basal lamina and SDD are subretinal and likely reflect activity along distinct pathways within polarized RPE [74]. The fovea is the region with the highest packing density of cones, and cone damage and destruction is an important consequence of late AMD. This is the first study to show that rods may play an important pathophysiologic stimulus for the development of AMD, due to the formation of SDD. A component of early AMD, SDD is a recognized risk factor for the development of both geographic atrophy and choroidal neovascularization.

Acknowledgments

Funding: NIH grants EY06109, International Retinal Research Foundation, Research to Prevent Blindness, Inc., EyeSight Foundation of Alabama.

References

1. Zweifel SA, Spaide RF, Curcio CA, et al. Reticular pseudodrusen are subretinal drusenoid deposits. Ophthalmology. 2010; 117:303–12e.1. [PubMed: 19815280]
2. Sarks JP, Sarks SH, Killingsworth MC. Evolution of geographic atrophy of the retinal pigment epithelium. Eye. 1988; 2:552–577. [PubMed: 2476333]
3. Sarks S, Cherepanoff S, Killingsworth M, Sarks J. Relationship of basal laminar deposit and membranous debris to the clinical presentation of early age-related macular degeneration. Invest Ophthalmol Vis Sci. 2007; 48:968–77. [PubMed: 17325134]
4. Curcio CA, Presley JB, Medeiros NE, et al. Esterified and unesterified cholesterol in drusen and basal deposits of eyes with age-related maculopathy. Exp Eye Res. 2005; 81(6):731–741. [PubMed: 16005869]
5. Rudolf M, Clark ME, Chimento M, et al. Prevalence and morphology of druse types in the macula and periphery of eyes with age-related maculopathy. Invest Ophthalmol Vis Sci. 2008; 49:1200–1209. [PubMed: 18326750]
6. Wolkow N, Song Y, Wu TD, et al. Aceruloplasminemia: retinal histopathologic manifestations and iron-mediated melanosome degradation. Archives of Ophthalmology. 2011; 129:1466–74. [PubMed: 22084216]
7. Rudolf M, Malek G, Messinger JD, et al. Sub-retinal drusenoid deposits in human retina: organization and composition. Exp Eye Res. 2008; 87:402–408. [PubMed: 18721807]
8. Mimoun G, Soubrane G, Coscas G. Macular drusen. J Fr Ophtalmol. 1990; 13:511–30. [PubMed: 2081842]
9. Spaide RF, Curcio CA. Drusen characterization with multimodal imaging. Retina. 2010; 30:1441–54. [PubMed: 20924263]
10. Arnold JJ, Sarks SH, Killingsworth MC, Sarks JP. Reticular pseudodrusen. A risk factor in age-related maculopathy. Retina. 1995; 15:183–191. [PubMed: 7569344]

11. Sarks J, Arnold J, Ho IV, et al. Evolution of reticular pseudodrusen. Br J Ophthalmol. 2011; 95:979–85. [PubMed: 21109695]
12. Curcio CA, Millican CL. Basal linear deposit and large drusen are specific for early age-related maculopathy. Arch Ophthalmol. 1999; 117:329–339. [PubMed: 10088810]
13. Curcio CA, Messinger JD, Mitra AM, et al. Human chorioretinal layer thicknesses measured using macula-wide high resolution histological sections. Invest Ophthalmol Vis Sci. 2011; 52:3943–54. [PubMed: 21421869]
14. Curcio CA, Medeiros NE, Millican CL. The Alabama age-related macular degeneration grading system for donor eyes. Invest Ophthalmol Vis Sci. 1998; 39:1085–1096. [PubMed: 9620067]
15. Curcio CA, Millican CL, Bailey T, Kruth HS. Accumulation of cholesterol with age in human Bruch's membrane. Invest Ophthalmol Vis Sci. 2001; 42:265–274. [PubMed: 11133878]
16. Guyton JR, Klemp KF. Ultrastructural discrimination of lipid droplets and vesicles in atherosclerosis: value of osmium-thiocarbohydrazide-osmium and tannic acid-paraphenylenediamine techniques. J Histochem Cytochem. 1988; 36:1319–1328. [PubMed: 2458408]
17. Curcio CA, Messinger JD, Sloan KR, et al. Basal linear deposit in non-neovascular age-related macular degeneration: natural history, volume, biomechanics. in preparation.
18. Spraul CW, Lang GE, Grossniklaus HE. Morphometric analysis of the choroid, Bruch's membrane, and retinal pigment epithelium in eyes with age-related macular degeneration. Invest Ophthalmol Vis Sci. 1996; 37:2724–2735. [PubMed: 8977488]
19. Sarks SH. Ageing and degeneration in the macular region: a clinico-pathological study. Br J Ophthalmol. 1976; 60:324–341. [PubMed: 952802]
20. Curcio CA, Allen KA. Topography of ganglion cells in human retina. J Comp Neurol. 1990; 300:5–25. [PubMed: 2229487]
21. Curcio CA, Sloan KR, Kalina RE, Hendrickson AE. Human photoreceptor topography. J Comp Neurol. 1990; 292:497–523. [PubMed: 2324310]
22. Vogt SD, Curcio CA, Wang L, et al. Retinal pigment epithelial expression of complement regulator CD46 is altered early in the course of geographic atrophy. Exp Eye Res. 2011; 93:413–423. [PubMed: 21684273]
23. Rudolf M, Vogt SD, Curcio CA, et al. Histological basis of variations in retinal pigment epithelium autofluorescence in eyes with geographic atrophy. Ophthalmology. 2012 Resubmitted 6/27/12.
24. Marmorstein LY, McLaughlin PJ, Peachey NS, et al. Formation and progression of sub- retinal pigment epithelium deposits in Efemp1 mutation knock-in mice: a model for the early pathogenic course of macular degeneration. Human molecular genetics. 2007; 16:2423–32. [PubMed: 17664227]
25. Ruberti JW, Curcio CA, Millican CL, et al. Quick-freeze/deep-etch visualization of age- related lipid accumulation in Bruch's membrane. Invest Ophthalmol Vis Sci. 2003; 44:1753–9. [PubMed: 12657618]
26. Huang JD, Presley JB, Chimento MF, et al. Age-related changes in human macular Bruch's membrane as seen by quick-freeze/deep-etch. Exp Eye Res. 2007; 85:202–218. [PubMed: 17586493]
27. Kuntz CA, Jacobson SG, Cideciyan AV, et al. Sub-retinal pigment epithelial deposits in a dominant late-onset retinal degeneration. Invest Ophthalmol Vis Sci. 1996; 37:1772–1782. [PubMed: 8759344]
28. Arnold JJ, Sarks JP, Killingsworth MC, et al. Adult vitelliform macular degeneration: a clinicopathological study. Eye. 2003; 17:717–26. [PubMed: 12928683]
29. Klein R, Davis MD, Magli YL, et al. The Wisconsin Age-Related Maculopathy Grading System. Ophthalmol. 1991; 98:1128–1134.
30. Curcio CA, Johnson M, Huang JD, Rudolf M. Aging, age-related macular degeneration, and the Response-to-Retention of apolipoprotein B-containing lipoproteins. Prog Ret Eye Res. 2009; 28:393–422.
31. McLeod DS, Lutty GA. High-resolution histologic analysis of the human choroidal vasculature. Invest Ophthalmol Vis Sci. 1994; 35:3799–811. [PubMed: 7928177]

32. Mullins RF, Johnson MN, Faidley EA, et al. Choriocapillaris vascular dropout related to density of drusen in human eyes with early age-related macular degeneration. Investigative ophthalmology & visual science. 2011; 52:1606–12. [PubMed: 21398287]
33. Johnson PT, Lewis GP, Talaga KC, et al. Drusen-associated degeneration in the retina. Invest Ophthalmol Vis Sci. 2003; 44:4481–8. [PubMed: 14507896]
34. van der Schaft TL, Mooy CM, de Bruijn WC, et al. Histologic features of the early stages of age-related macular degeneration. Ophthalmol. 1992; 99:278–286.
35. Green WR, Enger C. Age-related macular degeneration histopathologic studies: the 1992 Lorenz E. Zimmerman Lecture. Ophthalmology. 1993; 100:1519–1535. [PubMed: 7692366]
36. Kamei M, Hollyfield JG. TIMP-3 in Bruch's membrane: changes during aging and in age- related macular degeneration. Investigative Ophthalmology & Visual Science. 1999; 40:2367–75. [PubMed: 10476804]
37. Malek G, Li CM, Guidry C, et al. Apolipoprotein B in cholesterol-containing drusen and basal deposits in eyes with age-related maculopath. Am J Pathol. 2003; 162:413–425. [PubMed: 12547700]
38. Luibl V, Isas JM, Kayed R, et al. Drusen deposits associated with aging and age-related macular degeneration contain nonfibrillar amyloid oligomers. J Clin Invest. 2006; 116:378–85. [PubMed: 16453022]
39. Sarks SH, van Driel D, Maxwell L, Killingsworth M. Softening of drusen and subretinal neovascularization. Trans Ophthalmol Soc U K. 1980; 100:414–422. [PubMed: 6171074]
40. Curcio CA, Presley JB, Millican CL, Medeiros NE. Basal deposits and drusen in eyes with age-related maculopathy: evidence for solid lipid particles. Exp Eye Res. 2005; 80:761–775. [PubMed: 15939032]
41. Hageman GS, Mullins RF. Molecular composition of drusen as related to substructural phenotype. Mol Vis. 1999; 5:28–37. [PubMed: 10562652]
42. Zweifel SA, Imamura Y, Spaide TC, et al. Prevalence and significance of subretinal drusenoid deposits (reticular pseudodrusen) in age-related macular degeneration. Ophthalmology. 2010; 117:1775–81. [PubMed: 20472293]
43. Helb HM, Charbel Issa P, Fleckenstein M, et al. Clinical evaluation of simultaneous confocal scanning laser ophthalmoscopy imaging combined with high-resolution, spectral-domain optical coherence tomography. Acta Ophthalmol. 2010; 88:842–9. [PubMed: 19706019]
44. Sohrab MA, Smith RT, Salehi-Had H, et al. Image registration and multimodal imaging of reticular pseudodrusen. Investigative ophthalmology & visual science. 2011
45. Schmitz-Valckenberg S, Alten F, Steinberg JS, et al. Reticular drusen associated with geographic atrophy in age-related macular degeneration. Investigative ophthalmology & visual science. 2011; 52:5009–5015. [PubMed: 21498612]
46. Wang JJ, Mitchell P, Smith W, Cumming RG. Bilateral involvement by age-related maculopathy lesions in a population. Br J Ophthalmol. 1998; 82:743–747. [PubMed: 9924363]
47. Klein R, Meuer SM, Knudtson MD, et al. The epidemiology of retinal reticular drusen. Am J Ophthalmol. 2007; 145
48. Smith RT, Sohrab MA, Busuioc M, Barile G. Reticular macular disease. Am J Ophthalmol. 2009; 148:733–743 e2. [PubMed: 19878758]
49. Schmitz-Valckenberg S, Steinberg JS, Fleckenstein M, et al. Combined confocal scanning laser ophthalmoscopy and spectral-domain optical coherence tomography imaging of reticular drusen associated with age-related macular degeneration. Ophthalmology. 2010; 117:1169–1176. [PubMed: 20163861]
50. Querques G, Poitrine FC, Coscas F, et al. Analysis of progression of reticular pseudodrusen by spectral domain optical coherence tomography. Investigative Ophthalmology & Visual Science. 2012
51. Curcio CA, Johnson M, Rudolf M, Huang JD. The oil spill in ageing Bruch's membrane. Br J Ophthalmol. 2011; 95:1638–1645. [PubMed: 21890786]
52. Tserentsoodol N, Gordiyenko NV, Pascual I, et al. Intraretinal lipid transport is dependent on high density lipoprotein-like particles and class B scavenger receptors. Mol Vis. 2006; 12:1319–33. [PubMed: 17110915]

53. Barter PJ. Hugh Sinclair lecture: the regulation and remodelling of HDL by plasma factors. Atherosclerosis Supplements. 2002; 3:39–47. [PubMed: 12573362]
54. Asztalos BF, Tani M, Schaefer EJ. Metabolic and functional relevance of HDL subspecies. Current Opinion in Lipidology. 2011; 22:176–85. [PubMed: 21537175]
55. Vaisar T, Pennathur S, Green PS, et al. Shotgun proteomics implicates protease inhibition and complement activation in the antiinflammatory properties of HDL. J Clin Invest. 2007; 117:746–56. [PubMed: 17332893]
56. Yu CJ, Youmans KL, LaDu MJ. Proposed mechanism for lipoprotein remodelling in the brain. Biochimica et Biophysica Acta-Molecular and Cell Biology of Lipids. 2010; 1801:819–823.
57. Hayashi H. Lipid metabolism and glial lipoproteins in the central nervous system. Biol Pharm Bull. 2011; 34:453–461. [PubMed: 21467629]
58. Cramer PE, Cirrito JR, Wesson DW, et al. ApoE-directed therapeutics rapidly clear beta- amyloid and reverse deficits in AD mouse models. Science. 2012; 335:1503–1506. [PubMed: 22323736]
59. Chen W, Stambolian D, Edwards AO, et al. Genetic variants near TIMP3 and high-density lipoprotein-associated loci influence susceptibility to age-related macular degeneration. Proc Natl Acad Sci U S A. 2010; 107:7401–6. [PubMed: 20385819]
60. Neale BM, Fagerness J, Reynolds R, et al. Genome-wide association study of advanced age-related macular degeneration identifies a role of the hepatic lipase gene (LIPC). Proc Natl Acad Sci U S A. 2010; 107:7395–400. [PubMed: 20385826]
61. Yu Y, Reynolds R, Fagerness J, et al. Association of variants in the LIPC and ABCA1 genes with intermediate and large drusen and advanced age-related macular degeneration. Investigative Ophthalmology & Visual Science. 2011; 52:4663–70. [PubMed: 21447678]
62. Dudley PA, Anderson RE. Phospholipid transfer protein from bovine retina with high activity towards retinal rod disc membranes. FEBS letters. 1978; 95:57–60. [PubMed: 720607]
63. Shanmugaratnam J, Berg E, Kimerer L, et al. Retinal Muller glia secrete apolipoproteins E and J which are efficiently assembled into lipoprotein particles. Mol Brain Res. 1997; 50:113–120. [PubMed: 9406925]
64. Schneeberger SA, Iwahashi CK, Hjelmeland LM, et al. Apolipoprotein E in the subretinal fluid of rhegmatogenous and exudative retinal detachments. Retina. 1997; 17:38–43. [PubMed: 9051841]
65. Wong P, Pfeffer BA, Bernstein SL, et al. Clusterin protein diversity in the primate eye. Mol Vis. 2000; 6:184–91. [PubMed: 11054462]
66. Anderson DH, Ozaki S, Nealon M, et al. Local cellular sources of apolipoprotein E in the human retina and retinal pigmented epithelium: implications for the process of drusen formation. Am J Ophthalmol. 2001; 131:767–781. [PubMed: 11384575]
67. Ishida BY, Bailey KR, Duncan KG, et al. Regulated expression of apolipoprotein E by human retinal pigment epithelial cells. J Lipid Res. 2004; 45:263–271. [PubMed: 14594998]
68. Ebrahimi KB, Wang L, Tagami M, et al. Oxidized Low Density Lipoprotein-Induced Injury in RPE Cells Alters Expression of the Transmembrane Complement Regulatory Factors CD46 and CD59 through Exosomal and Apoptotic Bleb Release. Invest Ophthalmol Vis Sci. 53 E-Abstract 1650.
69. Dowhan, W.; Bogdanov, M. Functional roles of lipids in membranes. In: Vance, DE.; Vance, JE., editors. Biochemistry of Lipids, Lipoproteins and Membranes. Amsterdam: Elsevier; 2002. p. 1-35.
70. Boesze-Battaglia K, Fliesler SJ, Albert AD. Relationship of cholesterol content to spatial distribution and age of disk membranes in retinal rod outer segments. J Biol Chem. 1990; 265:18867–18870. [PubMed: 2229047]
71. Albert AD, Boesze-Battaglia K. The role of cholesterol in rod outer segment membranes. Progress in Lipid Research. 2005; 44:99–124. [PubMed: 15924998]
72. Bazan NG, Gordon WC, Rodriguez de Turco EB. Docosahexaenoic acid uptake and metabolism in photoreceptors: retinal conservation by an efficient retinal pigment epithelial cell-mediated recycling process. Adv Exp Med Biol. 1992; 318:295–306. [PubMed: 1386177]
73. Rodriguez de Turco EB, Parkins N, Ershov AV, Bazan NG. Selective retinal pigment epithelial cell lipid metabolism and remodeling conserves photoreceptor docosahexaenoic acid following phagocytosis. J Neurosci Res. 1999; 57:479–486. [PubMed: 10440897]

74. Curcio CA. Complementing apolipoprotein secretion by retinal pigment epithelium. Proc Natl Acad Sci U S A. 2011; 108:18569–70. [PubMed: 22065764]
75. Prenner JL, Rosenblatt BJ, Tolentino MJ, et al. Risk factors for choroidal neovascularization and vision loss in the fellow eye study of CNVPT. Retina. 2003; 23:307–14. [PubMed: 12824829]
76. Einbock W, Moessner A, Schnurrbusch UE, et al. Changes in fundus autofluorescence in patients with age-related maculopathy Correlation to visual function: a prospective study. Graefe's archive for clinical and experimental ophthalmology = Albrecht von Graefes Archiv fur klinische und experimentelle Ophthalmologie. 2005; 243:300–5.
77. Smith RT, Chan JK, Busuoic M, et al. Autofluorescence characteristics of early, atrophic, and high-risk fellow eyes in age-related macular degeneration. Invest Ophthalmol Vis Sci. 2006; 47:5495–504. [PubMed: 17122141]
78. Cohen SY, Dubois L, Tadayoni R, et al. Prevalence of reticular pseudodrusen in age- related macular degeneration with newly diagnosed choroidal neovascularisation. Br J Ophthalmol. 2007; 91:354–9. [PubMed: 16973663]
79. Wang JJ, Rochtchina E, Lee AJ, et al. Ten-year incidence and progression of age-related maculopathy: the Blue Mountains Eye Study. Ophthalmology. 2007; 114:92–8. [PubMed: 17198852]
80. Smith RT, Merriam JE, Sohrab MA, et al. Complement factor H 402H variant and reticular macular disease. Archives of Ophthalmology. 2011; 129:1061–6. [PubMed: 21825189]
81. Smailhodzic D, Fleckenstein M, Theelen T, et al. Central areolar choroidal dystrophy (CACD) and age-related macular degeneration (AMD): differentiating characteristics in multimodal imaging. Investigative Ophthalmology & Visual Science. 2011; 52:8908–18. [PubMed: 22003107]
82. Forte R, Querques G, Querques L, et al. Multimodal imaging of dry age-related macular degeneration. Acta Ophthalmol. 2012; 90:e281–7. [PubMed: 22269083]
83. Tserentsoodol N, Sztein J, Campos M, et al. Uptake of cholesterol by the retina occurs primarily via a low density lipoprotein receptor-mediated process. Mol Vis. 2006; 12:1306–18. [PubMed: 17110914]
84. Johnson, LV.; Forest, DL.; Banna, CD., et al. Cell culture model that mimics drusen formation and triggers complement activation associated with age-related macular degeneration. Proceedings of the National Academy of Sciences of the United States of America; 2011; p. 18277-82.
85. Elner VM. Retinal pigment epithelial acid lipase activity and lipoprotein receptors: effects of dietary omega-3 fatty acids. Trans Am Ophthalmol Soc. 2002; 100:301–38. [PubMed: 12545699]

Figure 1. Macula-wide, high-resolution section of an eye with non-neovascular AMD

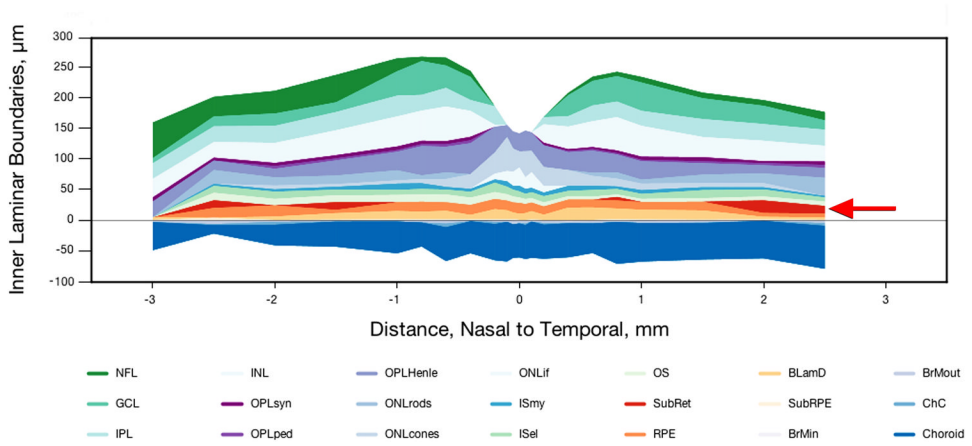

Figure 2. Histological layer thicknesses in non-neovascular AMD

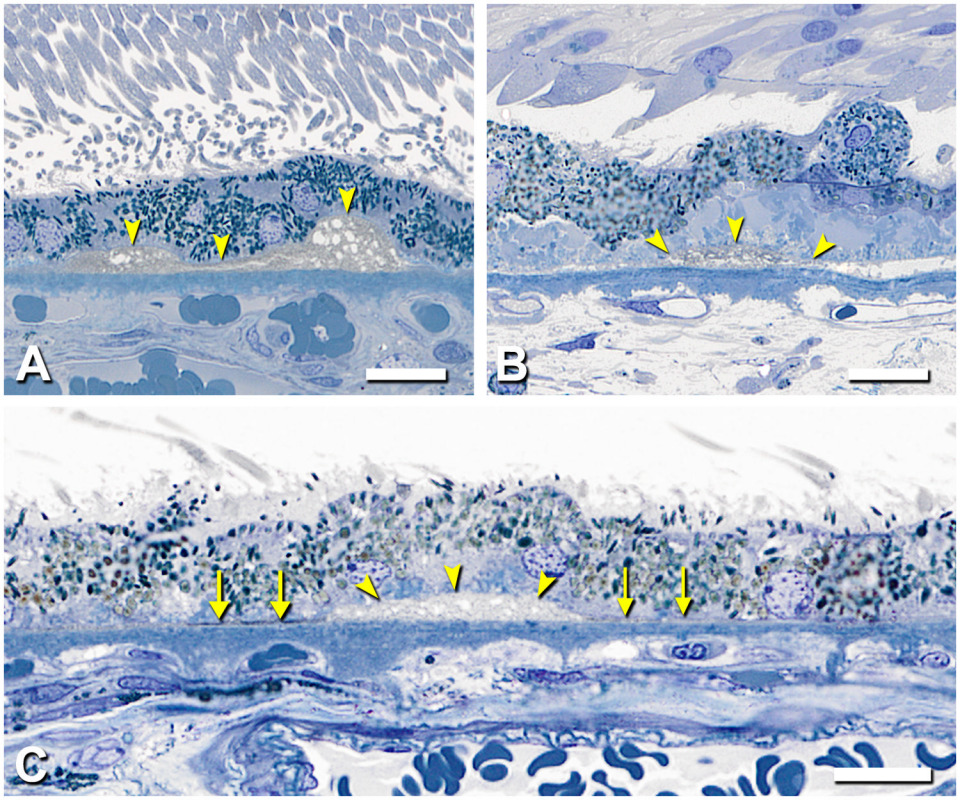

Figure 3. Basal linear deposits in atrophic AMD eyes

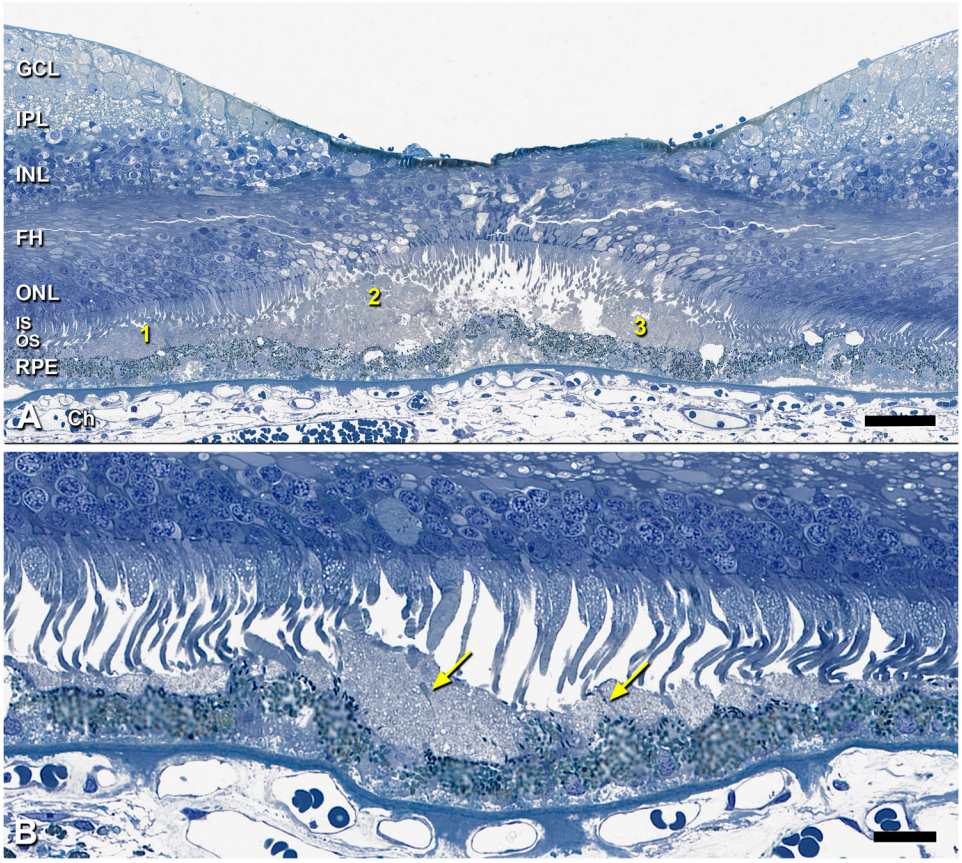

Figure 4. SDD morphology

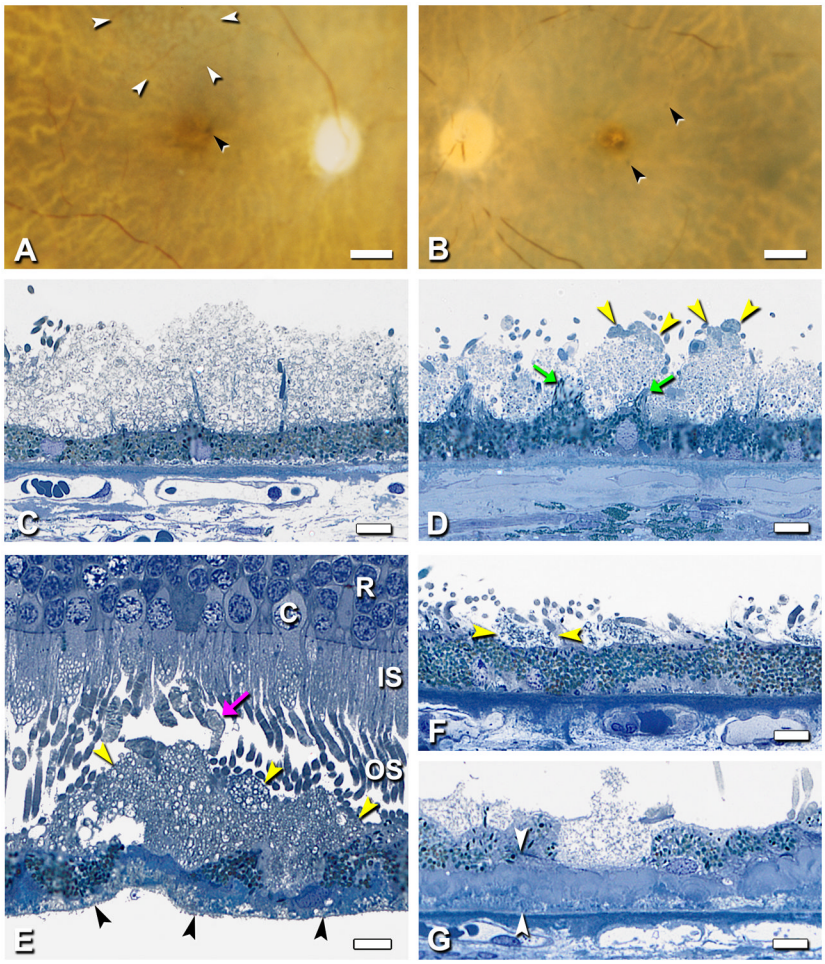

Figure 5. SDD in superior-temporal perifovea

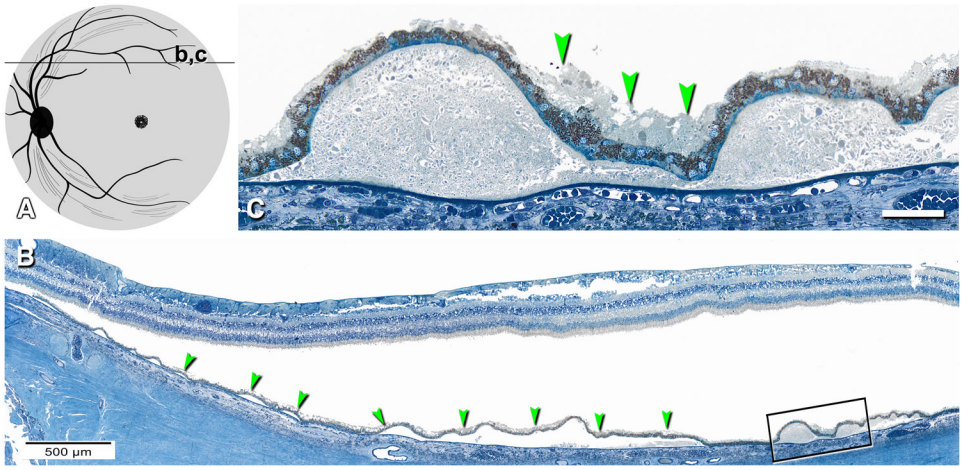

Figure 6. SDD is abundant in superior perifovea

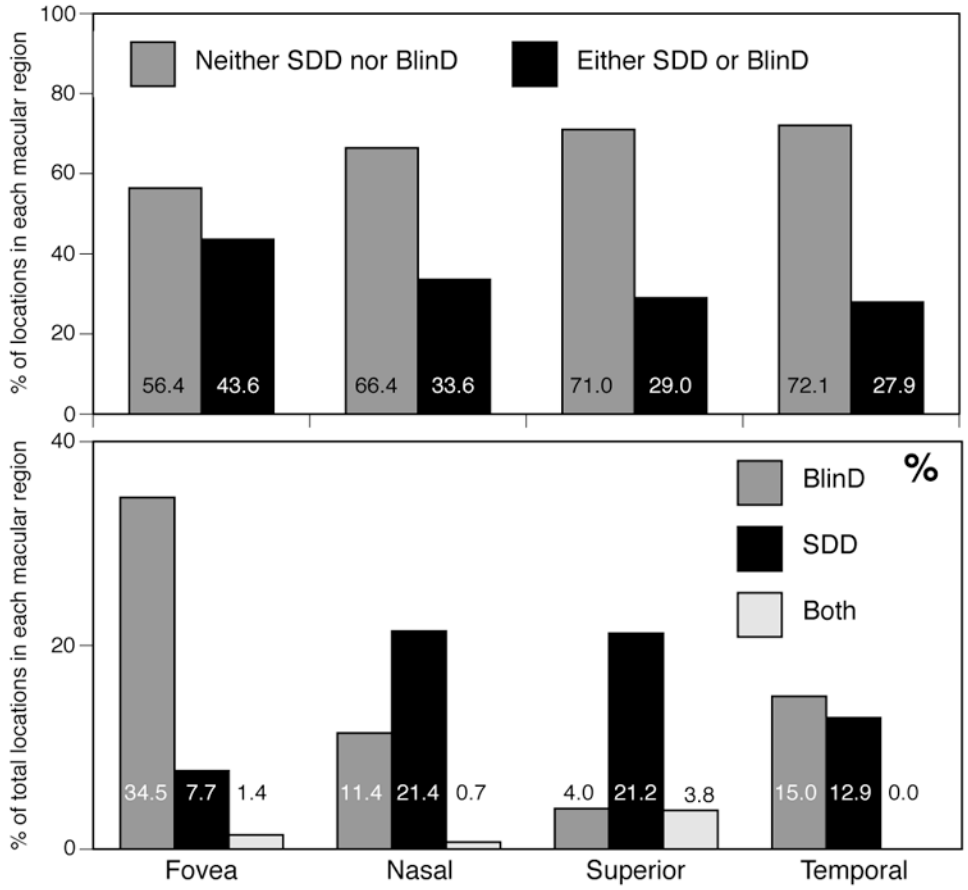

Figure 7. Prevalence of SDD and BlinD

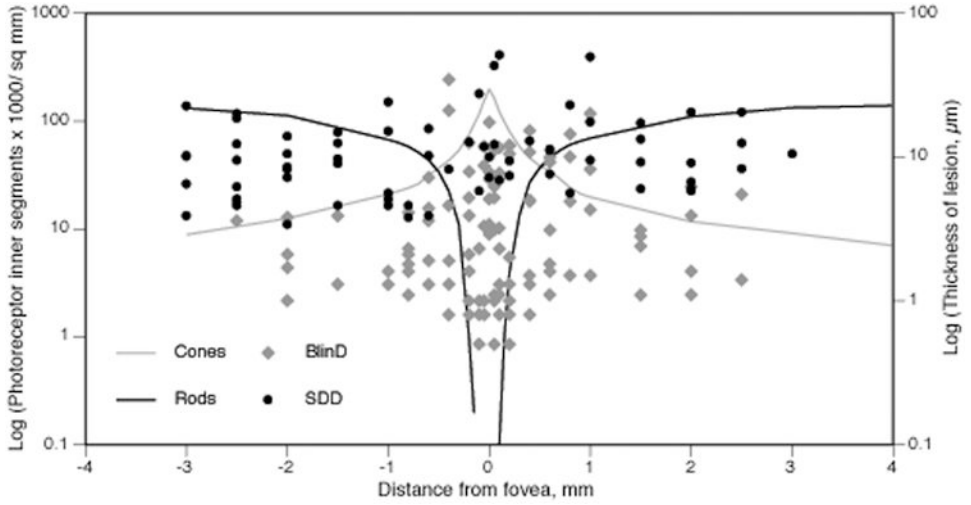

Figure 8. SDD and BlinD thicknesses and photoreceptor topography

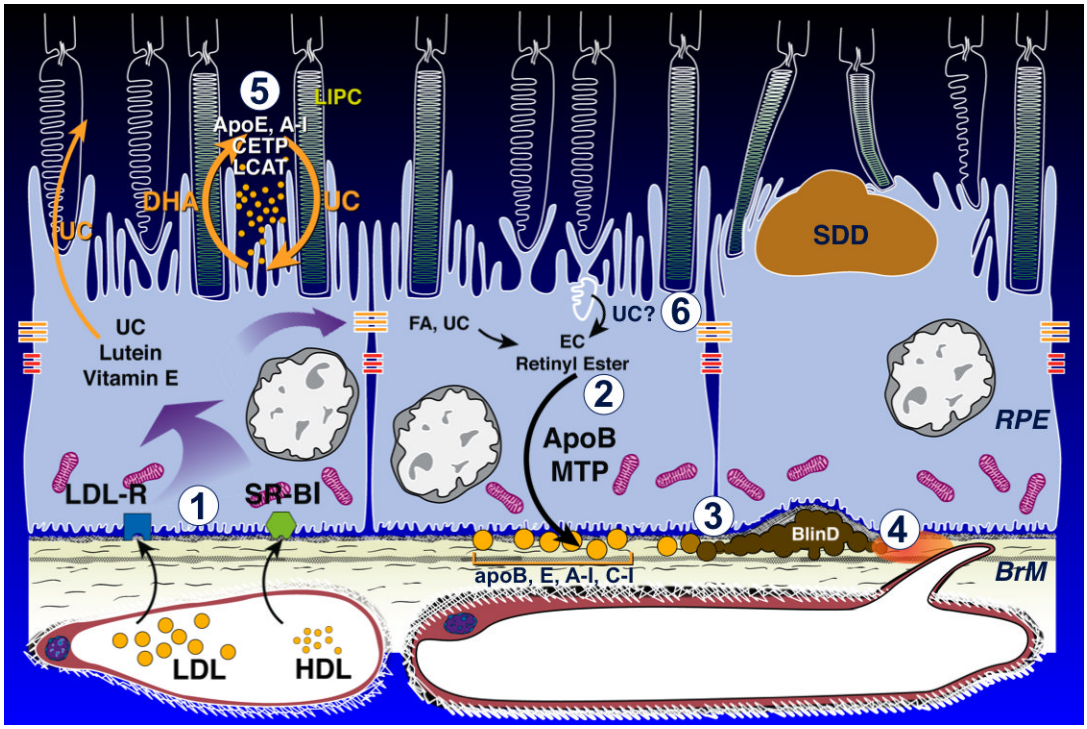

Figure 9. Biogenesis of sub-RPE and sub-retinal AMD lesions: model

Normal at left-center, AMD at right. Details in [1, 51]. OS, outer segment.. **BlinD, current 1**) Plasma lipoproteins delivering lipophilic nutrients enter RPE [83]. **2)** ApoB,E lipoproteins secreted basolaterally by RPE [84] (gold circles) are assembled from multiple lipid sources. Fatty acids are dominated by linoleate, implicating internalized plasma lipoproteins as a major source. UC from all sources is esterified to EC. **3)** Lipoproteins are retained by interacting with BrM extracellular matrix and accumulate throughout adulthood, creating a lipid wall on BrM's inner surface. **4)** Reactive oxygen species from neighboring mitochondria promote appearance of pro-inflammatory and toxic moieties. Lipoproteins fuse and form lipid pools and UC-rich liposomes within BlinD/ soft drusen, rendering them biomechanically unstable. **SDD, new 5)** Disks in rod OS lose UC and gain docosahexaenoate in transit from OS base to tip [71] (shown as loss of white). OS-derived DHA stored as triglycerides in RPE after phagocytosis return to OS [73]. HDL particles cycling between RPE and photoreceptors [52] could handle both transfers as part of a vectorial lipid flow retainable within interphotoreceptor matrix as UC-containing SDD, especially under rod-rich perifovea. **BlinD, new 6)** Cone OS maintain high UC content along their length, because their disks are comb-like projections of plasma membrane [71]. Cone OS UC enters RPE via disk shedding, lysosomal uptake, and acid lipase activity [85]. UC is released for intracellular transfer, esterification, and assembly into basolaterally-secreted lipoproteins, especially under cone-rich fovea.

Retina. Author manuscript; available in PMC 2014 February 01.

Table 1

SDD and BlinD morphometrics and histological associations at sampling locations

	Neither Lesion		SDD only		BlinD only		SDD+BlinD	
Macular subregion	#	%	#	%	#	%	#	%
Fovea	124	18.4	17	9.9	76	57.1	3	13.0
Nasal	93	13.8	30	17.5	16	12.0	1	4.4
Superior	355	52.8	106	62.0	20	15.0	19	82.6
Temporal	101	15.0	18	10.5	21	15.8	0	0.0
Perifovea (N+S+T)	549	81.6	154	90.1	57	42.9	20	87.0
All regions (F+N+S+T)	673	67.3	171	17.1	133	13.3	23	2.3
p<0.0001 for Fovea vs Nasal, Superior, and Temporal; Fovea vs Perifovea								
	Neither Lesion		SDD only		BlinD only		SDD+BlinD	
RPE pathology grade	#	%	#	%	#	%	#	%
0,1 (normal aging)	107	30.4	47	27.8	30	23.1	1	4.4
2 (very heterogeneous)	114	32.4	96	56.8	52	40.0	16	69.6
2A,2B,2L (reactive)	57	16.2	17	10.1	24	18.5	5	21.7
3 (intra-retinal)	32	9.1	8	4.7	5	3.9	0	0.0
4,5 (atrophic with and without BlamD)	42	11.9	1	0.6	19	14.6	1	4.4
p<0.0001 for differenc among lesion groups; p=0.0036 for SDD only vs BlinD only, grade 4-5 vs grade 0,1								
	Neither Lesion		SDD only		BlinD only		SDD+BlinD	
BlamD thickness	#	µm	#	µm	#	µm	#	µm
	673	5.22±6.05	171	4.22±4.03	133	6.20±5.52	23	4.75±3.77
p<0.03 for differences among lesion groups								
	Neither Lesion		SDD only		BlinD only		SDD+BlinD	
Choriocapillaris	#	%	#	%	#	%	#	%
No ghost	621	92.3	150	87.7	110	82.7	21	91.3
Ghost	52	7.7	21	12.3	23	17.3	2	8.7
p<0.0001 for differences between Neither and SDD only, BlinD only								

Notes: number of sampling locations in 4 lesion groups in 22 eyes is 673, 171, 133, and 23 for Macular Subregions, BlamD, and Choriocapillaris, and 352, 169, 133, and 23 for RPE RPE pathology grades adapted from [22, 23]: 0: uniform pigmentation and morphology; 1: non-uniform morphology and pigmentation; 2: very non uniform morphology and pigmentation but still epithelioid 2A: rounding and sloughing of individual cells from the underlying substrate (either Bruch's membrane or a layer of basal deposits); anterior migration of cells within the sub-retinal space; 2B: pigmented cellular fragments

within basal laminar deposit; 2L: double layer of continuous RPE; 3: anterior migration through the external limiting membrane and into neurosensory retina; 4: loss of pigmented cells with persisting basal laminar deposits; 5: absence of pigmented cells and basal laminar deposit

Table 2
Clinical studies reporting reticular drusen/SDD prevalence (chronological order)

Reference	Patient population (a)	Imaging modality	% affected
10	Newly presenting AMD cases	Various	13.0%
75	Non-AMD fellow eye	Red-free	3.0%
76	AMD		20.0%
77	Early AMD; non-neovascular AM	D FAF-SW	8.4%
77	CNV	FAF-SW	36.0%
78	Exudative AMD		24.0%
79	Population based; >80 yr	Color fundus photos (b)	30.0%
47	Population based; 75-86 yr	Color fundus photos	2.4%
42	Late AMD	SD-OCT	33.0%
45	Geographic atrophy	FAF-SW	55.7%
45	Geographic atrophy	IR reflectance	59.1%
80	Geographic atrophy	Various	91.0%
81	Geographic atrophy	FAF-SW	92.3%
82	Atrophic AMD	FAF-SW, FAF-NIR	29.0%

Notes: (a), as described by authors; FAF-SW = fundus autofluorescence, short wavelength (488 nm excitation); FAF-NIR = fundus autofluorescence, near infrared (830 nm excitation); (b) combined with indistinct drusen